HETEROJUNCTION BIPOLAR TRANSISTORS FOR MICROWAVE AND MILLIMETER-WAVE INTEGRATED CIRCUITS

P.M. Asbeck, M.F. Chang, K.C. Wang, D.L. Miller, G.J. Sullivan, N.H. Sheng, E.A. Sovero and J.A. Higgins

Rockwell International Corporation
Science Center
Thousand Oaks, CA 91360

ABSTRACT

This paper reviews the present status of GaAlAs/GaAs HBT technology and projects the impact of these devices on microwave and millimeter-wave integrated circuits. Devices with f_{max} above 100 GHz are described. Differential amplifiers are shown to have offset voltages with standard deviation below 2 mV and voltage gain of 200 per stage. Breakdown voltages (BV_{CBO}) above 20 V are demonstrated. Frequency dividers operating above 20 GHz are described.

I. INTRODUCTION

Prior to the advent of GaAs, microwave transistors were predominantly bipolar devices. With the development of heterojunction bipolar transistors (HBTs), bipolars deserve a new look.

Figure 1 illustrates a representative HBT cross section; its corresponding band diagram along the direction of electron travel is shown in Fig. 2.

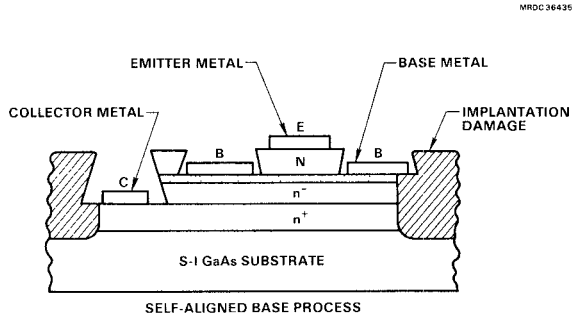

Fig. 1 Cross section of representative npn HBT.

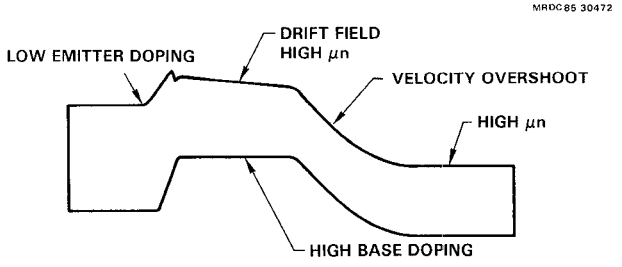

Fig. 2 HBT energy band diagram (npn).

HBTs based on III-V materials have a number of inherent advantages over Si bipolars, including the following[1]:

- Due to the wide bandgap emitter, a much higher base doping concentration can be used, decreasing base resistance.
- Emitter doping can be lowered, and minority carrier storage in the emitter can be made negligible, reducing base-emitter capacitance.
- High electron mobility, built-in drift fields and velocity overshoot combine to reduce electron transit times.
- Semi-insulating substrates help reduce pad parasitics and allow convenient integration of devices.
- Early voltages are higher and high injection effects are negligible due to the high base doping.

In comparison with FETs, HBTs also have many intrinsic advantages:

- The key distances that govern electron transit time are established by epitaxial growth, not by lithography, which allows high f_t with modest processing requirements.
- The entire emitter area conducts current, leading to high current handling capability and high transconductance.
- The "control region" of the device, the base-emitter junction, is very well shielded from the output voltage, leading to low output conductance; taken together with the high transconductance, enormous values of voltage amplification factor g_m/g_o are attainable.
- Breakdown voltage is directly controllable by the epitaxial structure of the device.
- The threshold voltage for output current flow is governed by the built-in potential of the base-emitter junction, leading to well-matched characteristics.
- The device is well shielded from traps in the bulk and surface regions, contributing to low 1/f noise, and absence of trap-induced frequency dependence of output resistance or current lag phenomena.

A variety of III-Vs are suitable for high-performance HBTs. This paper is primarily concerned with GaAlAs/GaAs heterostructures. Outstanding results are also emerging with InP or InAlAs/InGaAs lattice-matched to InP.

II. DEVICE TECHNOLOGY

With research efforts underway at more than 20 laboratories, HBT technology has progressed rapidly. Most of the work work has centered on MBE-grown structures, although attention is also being focused on MOCVD as the prospect of volume manufacturing nears. Table 1 details a representative HBT layer structure.

CH2478-6/87/0000-0001$01.00 © 1987 IEEE

Table 1

Representative HBT Layer Structure

Layer	Al Composition	Thickness (Å)	Doping (cm^{-3})
n^+ Cap	0	500	1×10^{19}
N Emitter	0-0.25-0	2000	5×10^{17}
p^+ Base	0	600	2×10^{19}
n^- Collector	0	7000	$3\text{-}6 \times 10^{16}$
n^+ Subcollector	0	6000	5×10^{18}
Semi-Insulating GaAs Substrate			

Recently, transistors with very high base doping ($1\text{-}2 \times 10^{20}$ cm^{-3}) have been demonstrated[2,3], leading to base sheet resistances in the range 100-200 Ω/square. A principal limiting factor is concentration-enhanced diffusion of the base dopant. Strained-layer GaInAs base regions have also been used, which may benefit from splitting of the light/heavy hole band degeneracy, as well as from increased electron velocity and greater emitter-base bandgap differences[4]. Fabrication approaches vary according to whether the base is contacted with the use of acceptor implantation and rapid thermal annealing, or by selective etching[5,6]. In both cases, a major developmental goal is a "self-aligned" process in which the active emitter area and the edge of the base and emitter contacts are all defined with the same photoresist pattern, with controllably small (0.1 μm) separations between the regions. This reduces the area of the device which contributes parasitic base resistance and base-collector capacitance without contributing to transconductance. Reactive Ion Etch-defined dielectric sidewalls, and InGaAs top (emitter) contacting layers are becoming widespread techniques. An additional technique to minimize extrinsic base-collector capacitance is to compensate the collector region under the base contact with a damage implant (e.g., protons).

As an example of present HBT technology, Fig. 3 shows a microphotograph of a millimeter-wave HBT fabricated at Rockwell with a self-aligned process based on selective etching and dielectric liftoff[3]. The emitter fingers are 1.2 μm x 9 μm; the structure was fabricated with conventional contact optical lithography.

SC39451

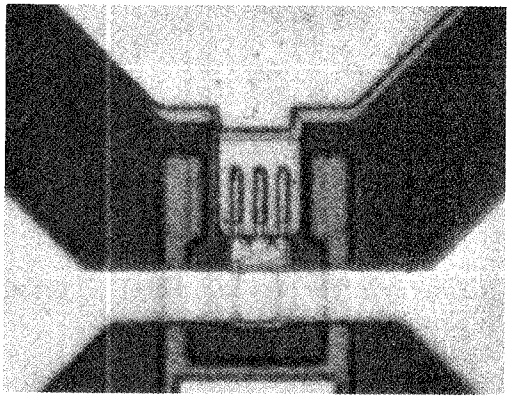

FULLY SELF-ALIGNED mm-WAVE HBT WITH 1.2 μm WIDE EMITTERS

Fig. 3 Microphotograph of HBT for millimeter-wave applications.

III. DEVICE CHARACTERISTICS

Figure 4 illustrates representative HBT common-emitter dc I-V characteristics. Transconductance increases with increasing collector current, reaching values of up to 5-10 mS/μm² of emitter area (corresponding to more than 10,000 mS/mm of emitter length with 1.2 μm wide emitters). Structures operate with current densities up to 10^5 A/cm² without current gain or cutoff frequency falloff. DC current gain, h_{fe}, is often a function of device size due to periphery recombination effects, although the effect is eliminated with graded bandgap bases[7] or appropriate AlGaAs edge passivation. Values in excess of 1000 have been reached, although h_{fe} near 10-20 is commonplace in the fastest devices. Breakdown voltage is typically high: Figures 5a and 5b show I-V characteristics on a high voltage scale for a device with 2.5 μm x 4.5 μm emitter in common-emitter and common-base operation, illustrating 15 V and 25 V breakdown voltages, respectively. In Fig. 5a, the negative output conductance is noteworthy - it results from device heating and decreasing current gain with temperature. Apart from the thermal and possible interpad leakage effects, output conductance is negligible. Early voltages are typically well above 100 V.

SC39692

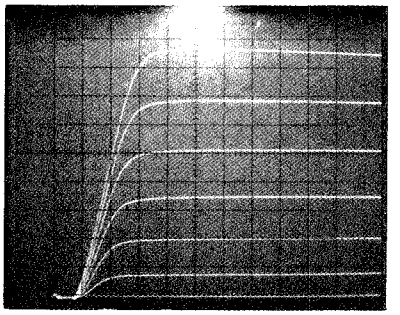

Fig. 4 I_c vs V_{ce} for an HBT with emitter dimensions 2.5 μm x 4.5 μm.

Figure 6 illustrates rf gain vs frequency, as calculated from S-parameters measured with a HP8510 network analyzer coupled with a Cascade probe system. The transistor corresponds to the device of Fig. 3, biased at I_c = 14 mA and V_{ce} = 1.4 V. A maximum frequency of oscillation, f_{max}, above 100 GHz may be extrapolated from the 1-26 GHz data, illustrating that HBTs can have useful gain well into the millimeter-wave frequency range (even with a minimum geometry of 1.2 μm). As shown in Fig. 7, S_{21} is remarkably high and S_{12} remarkably low over the entire range of the data, so that the devices are easy to match and to cascade. The calculated current gain h_{21} shown in Fig. 6 extrapolates to a cutoff frequency f_t of 55 GHz. Present record f_t performance corresponds to 68 GHz achieved by NTT.[8] Simulations suggest f_t = 150 GHz is possible.[9] A limitation to present HBTs is likely to be carrier storage in the emitter-base space-charge region.[10]

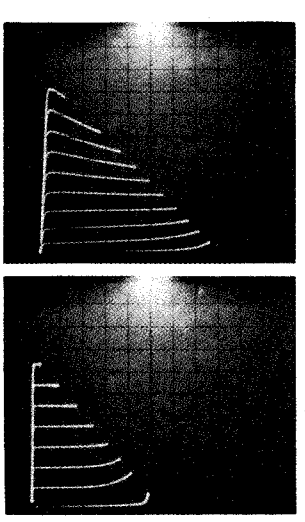

Fig. 5 I-V characteristics for device of Fig. 4 on high voltage scale: (a) common-emitter configuration; (b) common-base configuration.

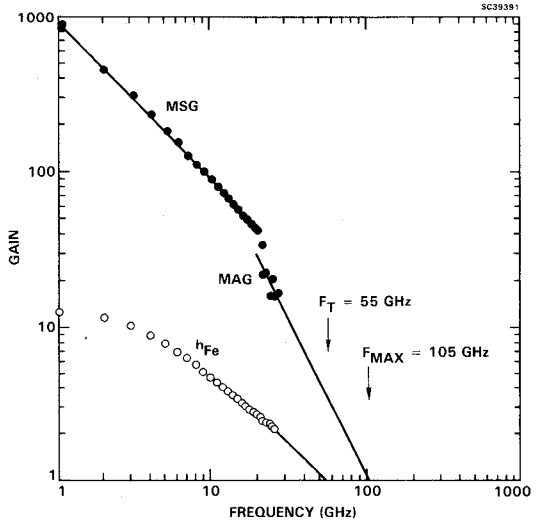

Fig. 6 Current gain, h_{21}, maximum available gain, MAG, and maximum stable gain, MSG, vs frequency for a millimter-wave HBT. Extrapolations at 6 dB/octave to f_t and f_{max} are shown.

Extensive noise measurements have not yet been done on millimeter-wave HBTs. Based on early measurements[11], it is believed that in the white noise regime, contributions from base current shot noise and base resistance Johnson noise are unlikely to allow noise figures to be competitive with state-of-the-art heterostructure FETs. In the 1/f noise regime, preliminary measurements[11] have shown noise corner frequencies below 1 MHz, a significant improvement over most FETs.

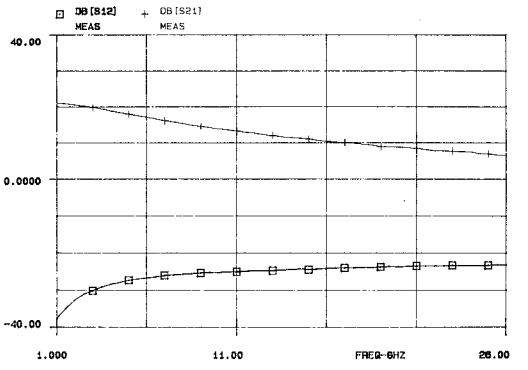

Fig. 7 Magnitudes of S_{21} and S_{12} vs frequency for the device of Fig. 6.

For analog/digital conversion and many other circuits, high current gain (> 50) is desirable. Figure 8 shows h_{fe} vs collector current for a Rockwell partially self-aligned device with 2 μm x 3.5 μm emitters. DC current gain up to 170 is evident, despite the small device size. The matching of these devices is a critical issue for many applications. Prototype differential amplifiers, as shown in Fig. 9a, distributed across a (small) wafer were measured. Figures 9b and 9c show histograms of the resulting input offset voltage and gain distributions, illustrating the excellent device matching obtained. A high voltage amplification factor is also evident if (external) high resistance loads are used. Figure 10 shows input-output dc transfer curves for a single differential amplifier showing a voltage gain of 200 (46 dB).

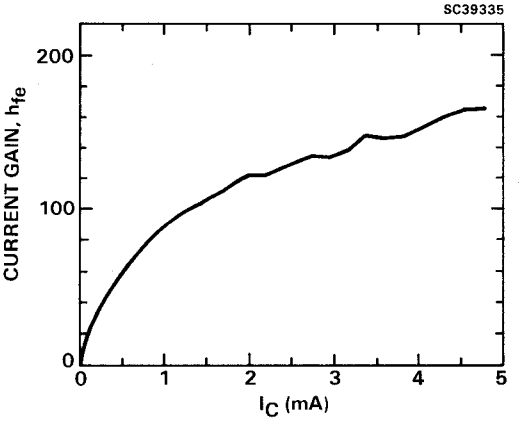

Fig. 8 Incremental dc current gain, h_{fe}, vs collector current for a 2 μm x 3.5 μm emitter device for digital and A/D applications.

IV. INTEGRATED CIRCUIT PROSPECTS

The application of HBTs in microwave and millimeter-wave ICs is in its early infancy. For the most part, the applications are envisioned to follow paths established by Si bipolar technology, extended to considerably higher frequency. Some of the most promising areas include:

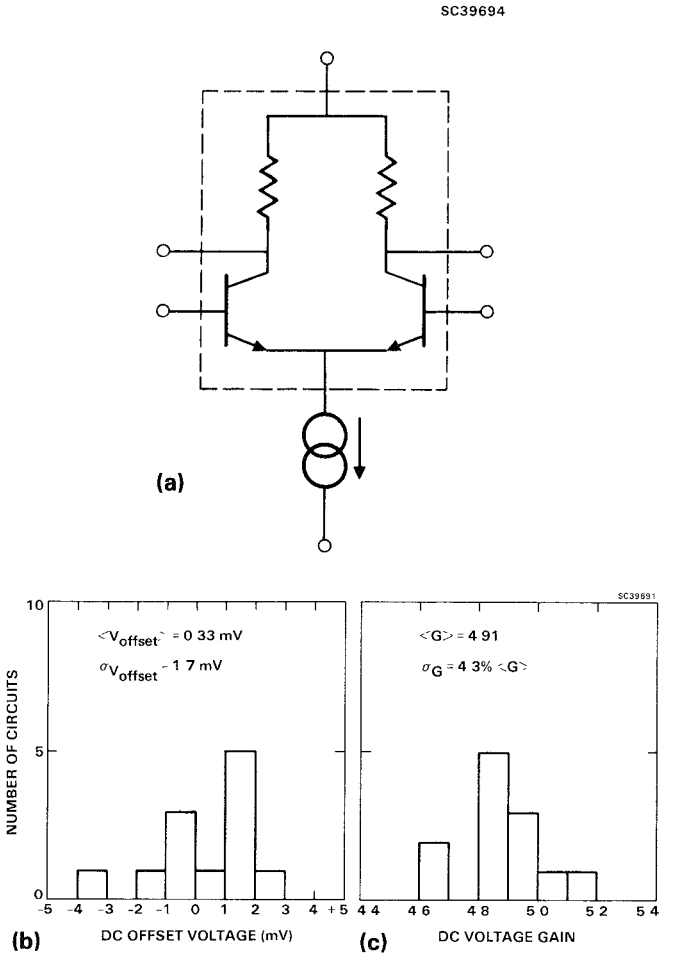

Fig. 9 (a) Prototype differential amplifier for device characterization; (b) histogram of measured input offset voltages across a small wafer; (c) histogram of corresponding voltage gain.

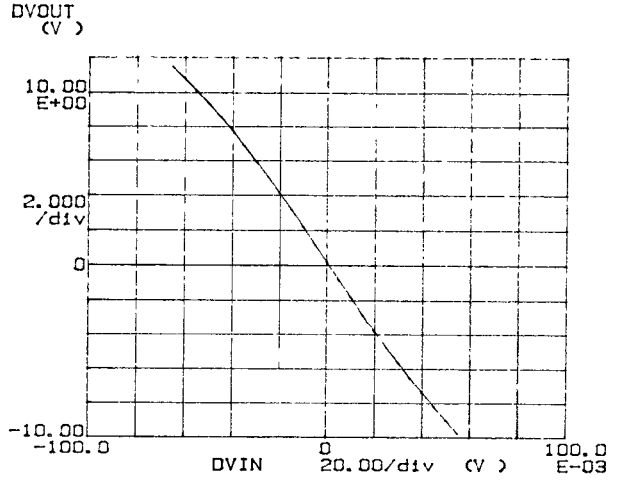

Fig. 10 Input-output voltage transfer curve for a single-stage differential amplifier showing gain of 200 (46 dB).

• Microwave power amplifiers of high efficiency. The high output breakdown voltage and current handling capability of HBTs can lead to high power in small chip areas. Class AB or Class C operation become convenient due to high gain and high breakdown voltages. The need for good heatsinking and possibly emitter ballasting are potential problems, although they are directly alleviated by pulsed operation. With discrete devices, initial demonstrations of pulsed Class C operation at 10 GHz have been done by Texas Instruments.[12] In Class A cw operation, 2.5 W per mm (thermally limited) at 12 GHz has also been reported.[11]

• Wideband analog circuits with frequency response from dc to 10 GHz. Use of feedback to obtain good control over gain and matching will be facilitated by high open-loop gain. As in lower frequency circuits, the inclusion of increasing numbers of active components and fewer large passive elements (inductors) will be favored. Low input offset voltages are available for dc coupling. Very good operational amplifiers should be possible. Nonlinear functions (AGC, log amps, multipliers) will be facilitated by the exponential input voltage output current characteristics of HBTs.

• Millimeter-wave amplifiers, primarily power amplifiers. Projected f_{max} values are above 200 GHz, particularly with inverted structure HBTs with the collector on the wafer surface for reduced collector feedback capacitance. The HBT is unique among candidate millimeter-wave devices in that it may be fabricated with conventional 1 μm optical lithography. Furthermore, HBTs are small enough that signal phase differences between different device regions are not a major concern as they are for FETs.

• Microwave oscillators with low phase noise based on the relatively low 1/f noise associated with HBTs. Using discrete device, Agarwal has shown FM noise of -73 dBc/Hz at 1 kHz separation from the carrier with a dielectric resonator-stabilized oscillator at 4 GHz[13].

• Analog/digital conversion. HBTs are particularly advantageous in the implementation of high-speed, high-accuracy comparators and flash converters due to their excellent input voltage matching, absence of hysteresis, and high speed.[14] HBT comparators have already been reported with offset error standard deviations on the order of 4 mV and 2.5 GSps operation.[15]

• Digital circuits. Digital techniques will be used in the future at frequencies considered heretofore exclusively analog. Frequency dividers are representative of maximum flip-flop toggling rate. With HBTs, static (master-slave) dividers have recently operated with up to 20.1 GHz input frequencies,[16] and further increases are expected. Millimeter-wave frequency dividers appear feasible.

V. SUMMARY

HBTs have copious current and power gain at microwave and millimeter-wave frequencies, and can be fabricated with straightforward optical lithography. Their current handling capability, input voltage dc matching, breakdown voltage and 1/f noise are potentially better than those for GaAs FETs. Based on these characteristics, HBTs are expected to have a bright future in microwave/millimeter-wave ICs.

VI. ACKNOWLEDGEMENTS

Rockwell portions of the work reported here were partially supported by DARPA and monitored by the Office of Naval Research. We are grateful to A. Gupta for many helpful conversations and assistance in measurements, and to L. Sullivan for assistance in wafer growth.

VII. REFERENCES

1. H. Kroemer, Proc. IEEE 70, 13 (1982).
2. J.L. Llevin, C. Dubon-Chevallier, F. Alexandre, G. Leroux, J. Dangla and D. Ankri, Electr. Dev. Lett. (1986).
3. M.F. Chang, P.M. Asbeck, K.C. Wang, N.H. Sheng, G.J. Sullivan and D.L. Miller (to be published).
4. G.J. Sullivan, P.M. Asbeck, M.F. Chang, D.L. Miller and K.C. Wang, Electr. Lett. 22, 419 (1986).
5. T. Izawa, T. Ishibashi and T. Sugeta, Tech. Digest 1985 IEDM, p. 328.
6. S. Tiwari, Tech. Digest 1986 IEDM, p. 262
7. H. Ito and T. Ishibashi, 1985 Int. Symp., GaAs and Related Compounds, Inst. Phys. Conf., Ser. No. 79, Ch. 11, p. 607.
8. H. Ito and T. Ishibashi (unpublished).
9. K. Tomizawa, Y. Awano and N. Hashizume, Electr. Dev. Lett. (1985).
10. N. Moll, Tech. Digest 1985 Cornell Conf.
11. P.M. Asbeck, A.K. Gupta, F.J. Ryan, D.L. Miller, R.J. Anderson, C.A. Liechti and F.H. Eisen, Tech. Digest 1984 IEDM, p. 846.
12. B. Kim and H.Q. Tserng (unpublished).
13. K. Agarwal, Tech. Digest 1986 MTT-S, p. 95.
14. K. deGraaf and K. Fawcett, Tech. Digest 1986 GaAs IC Symp., p. 205.
15. K.C. Wang, P.M. Asbeck, M.F. Chang, D.L. Miller and F.H. Eisen, Tech. Digest 1985 GaAs IC Symp., p. 99.
16. K.C. Wang, P.M. Asbeck, M.F. Chang, G.J. Sulliva and D.L. Miller (to be published).